Appl. Phys. A (2016) 122:390
DOI 10.1007/s00339-016-9952-7

Applied Physics A
Materials Science & Processing

Fabrication of alumina porous scaffolds with aligned oriented pores for bone tissue engineering applications

Fatemeh Sarhadi[1] · Mahdi Shafiee Afarani[1] · Davod Mohebbi-Kalhori[2] · Masoud Shayesteh[2]

Received: 16 November 2015 / Accepted: 29 February 2016 / Published online: 14 March 2016

Abstract In the present study, porous alumina scaffolds with specific orientation and anisotropic properties are fabricated for application in bone tissue repair. The scaffolds with double shape pores, tubular oriented and isotropic rounded pores, were prepared using alumina and silica as starting materials by the slip casting route. Milled polyurethane foam and silk fibers were applied as replica materials as well. The effect of fiber types and diameter and number of fibers on the microstructure and pore size was studied. Moreover, different characteristics such as porosity, density, orientation, flexural strength and compressive strength of the samples were investigated. Results showed that various fibers with different diameters and numbers led to forming the pores with different pore sizes, microstructure and consequently changes in the physical and mechanical properties. In addition, the simultaneous presence of fibers and particles led to more porous scaffolds. The oriented tiny micro-tube and rounded pores were observed in all porous ceramic scaffolds. Mechanical testing showed an anisotropy in the mechanical behaviors such that higher strengths were observed in the oriented pore direction than that of transverse. With increasing the number and diameter of silk fibers, the scaffolds with a high porosity up to 68 vol% and proper flexural strength were obtained.

✉ Mahdi Shafiee Afarani
shafieeafarani@gmail.com; shafiee@eng.usb.ac.ir

Fatemeh Sarhadi
f.sarhadi@pgs.usb.ac.ir

Davod Mohebbi-Kalhori
davoodmk@eng.usb.ac.ir

Masoud Shayesteh
shayeste@hamoon.usb.ac.ir

[1] School of Materials Engineering, Faculty of Engineering, University of Sistan and Baluchestan, Zahedan, Iran

[2] School of Chemical Engineering, Faculty of Engineering, University of Sistan and Baluchestan, Zahedan, Iran

1 Introduction

To date, several biocompatible scaffolds have been fabricated for application in bone tissue repair. However, there remains a need for development and synthesis of novel scaffolds in order to repair long bones in terms of segmental defects using biocompatible and durable materials during the patient lifetimes. In this regard, engineered custom metal augments and bone allografts are applied to repair segmental skeletal deficiency [1]. It should be noted that treatments are limited by three important factors by means of limited availability, unpredictable long-term durability and high cost. Aforementioned biocompatible scaffolds that replicate the structure and function on bone tissue should be ideal bone substitutes [1, 2]. This means they should be able to present mechanical properties for reliable long-term cyclical loading during weight bearing. The biocompatible scaffold should also be acceptable in terms of mechanical properties (e.g., compressive strength and elastic modulus) when compared to those of the native bone tissue to be replaced. In addition, the biocompatible scaffolds should present a microstructure and microenvironment for cell growth in initial step and tissue growth in next step within the porous scaffold, to provide formation of strong bonding and facilitation of integration with apposing host hard bone and surrounding soft tissue. A porosity of about 50 % (even more) and an interconnected pore size of about 100–300 μm are required in order to provide high surface area for cell interaction and sufficient

space for extracellular matrix regeneration and permit tissue in-growth and function [1, 3].

In addition, the ability to design of the biocompatible scaffolds with oriented tubular pores and porosities in 3D structures in order to use for the bone nerve and vascularized tissue engineering is one of the important and critical steps in regenerative medicine [4–6].

Moreover, the porous ceramics are finding increasing applications in various fields such as catalyst supports, hot gas collectors, filters, sensors, separation membranes and especially bone replacement [7–10]. Physical and mechanical properties of the porous ceramics are affected strongly with the sintering temperature, various additives and the type and pore former concentration. Different methods can be used for fabrication of the porous ceramic materials, such as the slip casting, compaction of powders with low applied pressure, vibration accomplished with partial sintering, sponge replica, sacrificial template, direct foaming, extrusion method and freeze drying [11–18].

The anisotropic nature of the porous alumina ceramics is an important feature in the applications that requires the open and aligned porous structures, such as bone tissue scaffolds, catalysts and membranes [19, 20]. Numerous studies have performed for fabrication of the structures with oriented/aligned pores by various methods such as the freeze drying and extrusion [11, 21, 22]. The orientation of pores in the bone tissue engineering scaffolds improves the mechanical properties in oriented pore direction compared to that of non-oriented scaffolds such as compressive and flexural strengths [23–26].

Although there are several open-literature investigations on the fabrication of the porous alumina supports and scaffolds, to the best of authors' knowledge, a few reports on the orientation of the pores were observed. The aim of the present work was fabrication of alumina porous scaffolds with bimodal structure having aligned oriented/isotropic pores via the integration of silk fiber and milled polyurethane particles by slip casting method. In addition, study on the physical and mechanical properties of the scaffold for bone tissue engineering applications was represented as well.

2 Experimental procedure

High-purity α-Al_2O_3 primary particles (WDR4, indal chemical, $d_{50} = 1$ μm, BET surface area 1.5 $m^2\ g^{-1}$ and a purity of 99.4 %) and SiO_2 powder (SYLOID AL-1FP, Grace Company, $d_{50} = 1$ μm, purity of 99 %) were used as the starting materials. Tiron (Aldrich 89460) was employed as dispersant. The silk threads with three different diameters of ~150, 400 and 600 μm that were formed using primary silk fibers of ~50 μm in diameter were used as the fugitive fiber to produce pores unidirectional aligned. To achieve the desired porosity in ceramic body, various experiments were performed. For this purpose, milled polyurethane foam (150–600 μm) was used as bulk pores former. Distilled water and pure hydrogen peroxide (H_2O_2, Dr. Mojallali Co., 35 vol%) were used as the slurry media. Hydrogen peroxide was selected as slurry media for its considerable gas removal during the thermal treatment. The slurries with composition of 59.9 wt% alumina, 3.15 wt% silica, 1.95 wt% milled polyurethane foam and 35 wt% hydrogen peroxide were prepared in a planetary mill (polyethylene cup and alumina balls) with rotational speed of 180 rpm for 30 min. For the stability of the slurry, 0.067 g Tiron dispersant was added to 100 g solid contents. The silk fibers were cleaned with acetone to remove from pollutions and aligned oriented in the homemade plaster mold with dimensions of 40 × 20 × 12 mm^3 (Fig. 1a, b), and the resulting slurry was injected into the mold. Then, the semi-dried samples were removed after remaining in the mold for 8–10 h. The obtained green bodies (after drying and before sintering) were slowly dried at room temperature for 24 h and then sintered at 1450 °C for 2 h in an electric furnace (Carbolite RHF 15). To prevent the

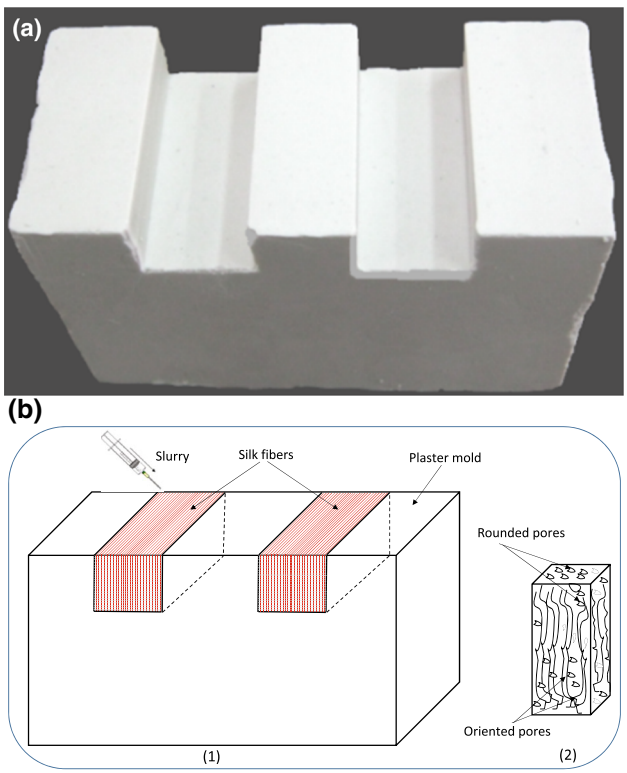

Fig. 1 **a** Macroimage of plaster mold and **b** schematic of the procedure utilized for preparing the scaffolds (*1*) aligned and directed silk fibers was placed inside the plaster mold, and the slurry was injected into the mold. (*2*) Scaffold with double pore shape architecture

green body from cracking during the burnout process of the silk fibers and milled polyurethane foam, a slow heating rate was adopted at low temperatures according to profile represented in Fig. 2.

Density and relative porosity of the samples were determined using mass and dimension measurements, considering theoretical density of Al_2O_3 as 3.985 g cm^{-3}. The surface area of scaffolds was determined by BET technique using a BELSORP-mini II instrument. Compressive strengths of the scaffolds were measured with a mechanical testing machine (INSTRON 4206) under a strain rate of 0.5 mm/min. The three-point flexural strengths of scaffolds in the direction perpendicular to the aligned oriented pores were measured by a mechanical testing machine (INSTRON 4206). Microstructure analysis of scaffolds was performed using a scanning electron microscopy (LEO 1455VP). The pore size distributions of the scaffolds were determined using Image J 1.44p, the image processing software.

All experiments were performed at least three times. Results are presented as the mean ± SD.

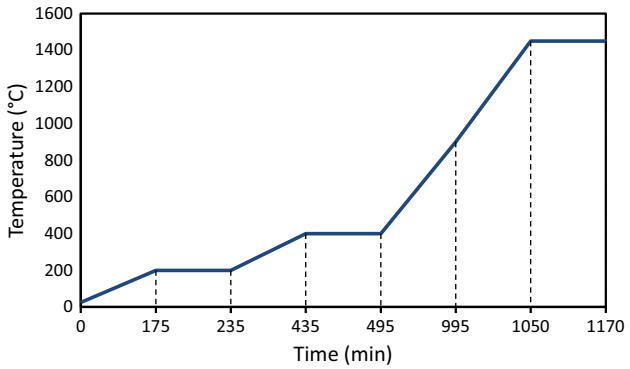

Fig. 2 Temperature profile of the sintering

3 Results and discussion

Porous alumina scaffold could be produced by the slip casting route by integration of the milled polyurethane foam and silk fibers as replica materials. Summary of the primary experiments is listed in Table 1. As illustrated, integration of simultaneous silk fibers and milled polyurethane foams, using hydrogen peroxide as slurry media, results in the scaffolds with appropriate strength and high porosity (experiment no. 6). Figures 3 and 4 show the SEM micrographs of the sintered scaffolds with different fibers diameter in transverse and aligned direction of the pores, respectively. As shown, two kinds of pores, axially oriented tiny micro-tube pores (TP) and bulk distributed rounded pores (RP), were formed and homogeneously distributed throughout the bulk of the samples. Moreover,

Table 1 Results summary of the primary experiments

	State	Method	Explanation
1	Dipping of replica and sacrificial templates into the slurry	Polypropylene fibers were passed through the polyurethane sponges with the pore density of 53ppi	Low strength and collapsed samples due to considerable organic removal
2	Slip casting in the presence of sacrificial templates	Aligned and directed polypropylene fibers were placed inside the plaster mold followed with the slip casting	Considerable macrocracking after drying and before sintering due to a dramatic difference of the expansion coefficients of the alumina and integrated polypropylene fibers
3		Polyvinylpyrrolidone (PVP) addition as surfactant for the better adhesion and wet ability	Considerable macrocracking after sintering due to a dramatic difference of the expansion coefficients of the alumina and polypropylene fibers
4	Slip casting in the presence of different kinds of fibrous sacrificial templates	Various fibers such as cotton, wool, nylon, silk and hemp were used as sacrificial templates	Nylon usage led to a considerable macrocracking after sintering due to a dramatic difference of their expansion coefficients. The cotton, hemp and wool had terrible residual ash after burning. Just applying the silk fibers results to crack free and moderate porosity. Not enough porosity (~45 %)
5	Use of simultaneous silk fibers and milled polyurethane foams	Polyurethane foams as sacrificial templates were milled and added to the alumina slurry	Not enough porosity (~50 %)
6	The presence of the silk fibers and milled polyurethane foams, using the hydrogen peroxide as slurry media	Alumina particles and milled polyurethane foams were suspended in the hydrogen peroxide as slurry media and then was poured into the mold containing silk fibers	Appropriate strength and high porosity (~70 %)

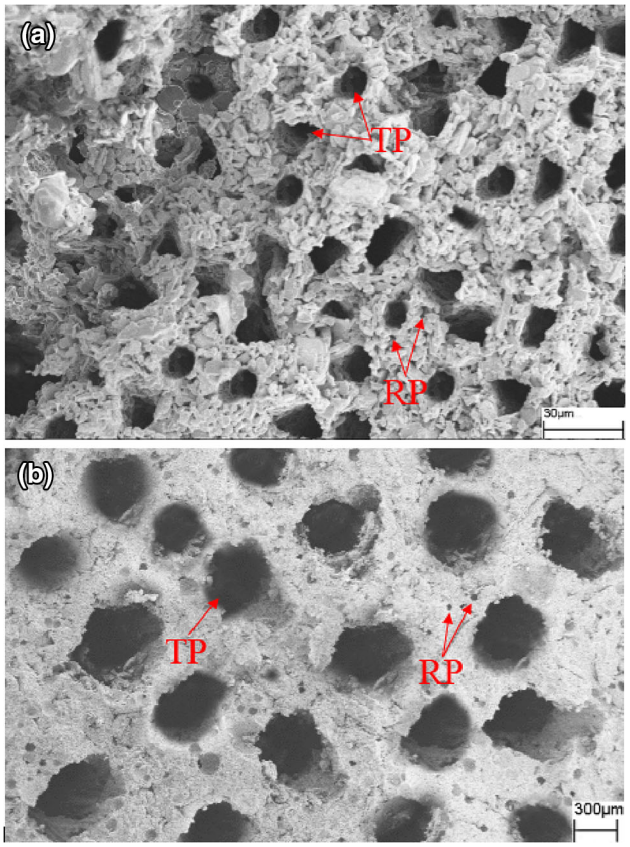

Fig. 3 Samples cross-section SEM micrographs in the transverse pore direction prepared with different fibers diameter of **a** ~150 μm and **b** ~600 μm

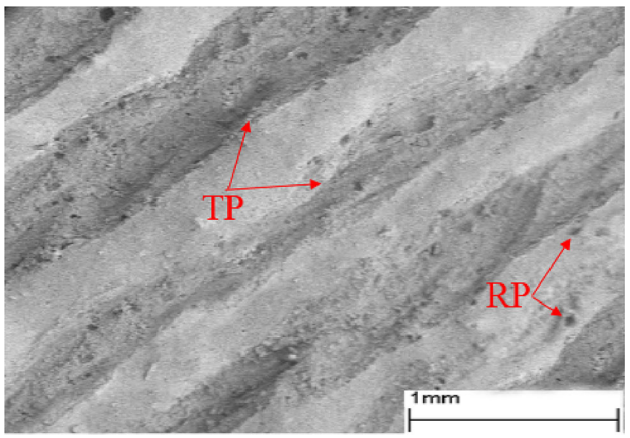

Fig. 4 SEM micrographs of the scaffold cross section in the oriented pore direction prepared with the fibers diameter of ~600 μm

obtaining pores with rough surfaces could increase specific surface area of samples (Fig. 5). This feature is an advantage for the use in bone tissue engineering because the mechanism of tissue attachment is directly related to the type of the tissue reaction at the tissue-scaffold

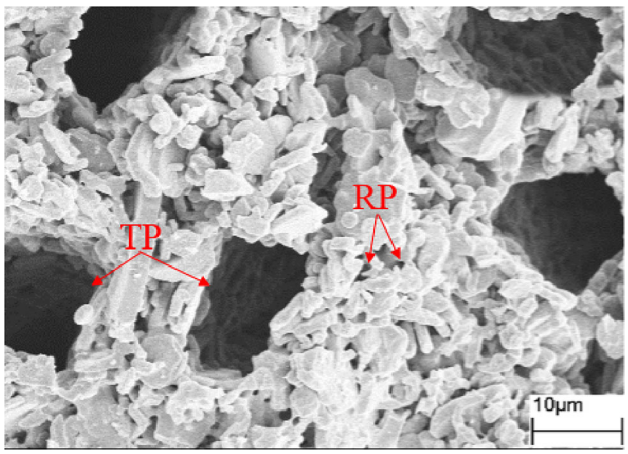

Fig. 5 SEM micrographs of the scaffolds with the aligned oriented and rounded pores

interface, as more surface roughness leads to less movement of the construct in the tissue as well as providing a blood supply to the connective ingrown tissue [5]. Furthermore, liquid-state sintering (i.e., smooth edge of particles) was observed due to silica presence as glassy aluminosilicate phase.

Figure 6 shows the pore size distribution of the scaffolds as a function of fibers diameter with number of 90–100. Broad pore distributions of samples are due to difference between the size of fibers and polyurethane particles and also oxygen gas removal from hydrogen peroxide. As shown, by increasing the diameter of the fiber, pore size distribution is shifted toward pores with a larger diameter. Considering SEM micrographs (Figs. 3, 5) and the pore size distribution (Fig. 6), macropores (100–600 μm) can promote the bone cells transplantation and micropores (<10 μm) may influence liquid and ions are required for the construction of artificial bone [24, 26].

A continuous trend of the density decrease and porosity increase as a function of the fibers diameter with number of 90–100 and numbers with 400 μm of diameter is shown in Fig. 7a, b. Moreover, using the hydrogen peroxide as a slurry media (instead of water) and milled polyurethane foam addition led to more porous bodies. It is due to decomposition of the hydrogen peroxide and oxygen gas removal for the earlier and organic removal for the latter during the sintering process. The simultaneous using of the hydrogen peroxide media and milled polyurethane foam represented scaffolds with considerable porosity up to about 70 vol% and density to about 1.45 g cm^{-3}. Similar behavior may also be observed in the porosity and density versus the number of fibers (Fig. 8a, b), respectively. As expected, increasing the number of fibers improved the volume fraction of the burned species, and consequently, the scaffolds with higher porosity and lower density were

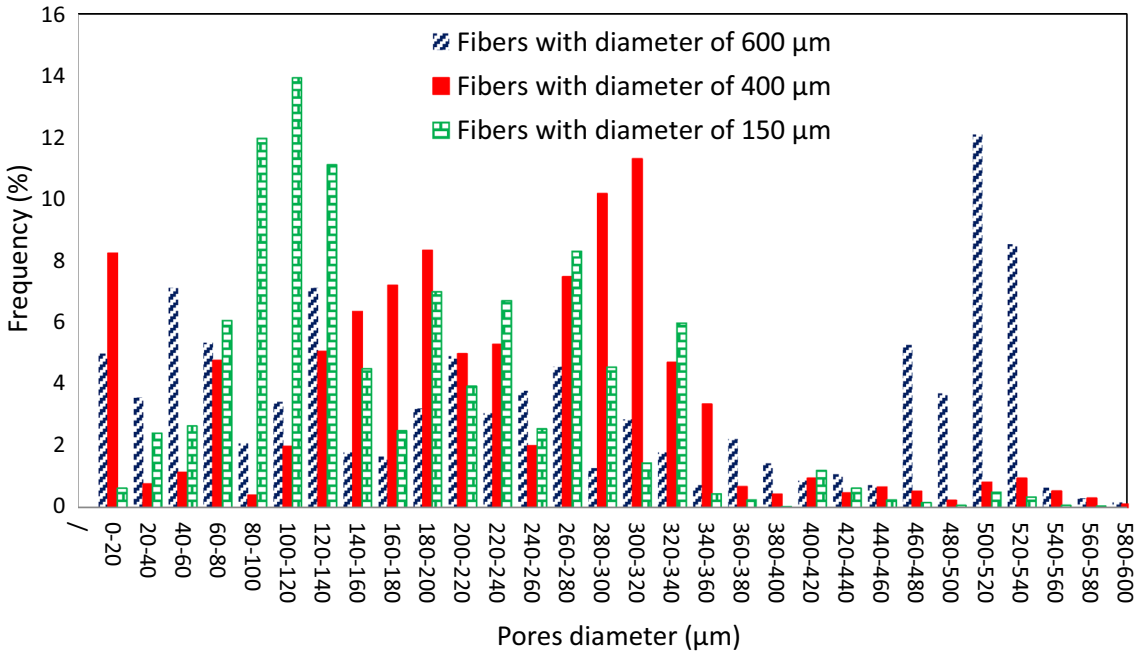

Fig. 6 Pore size distribution of the scaffolds as a function of the fibers diameter with 90–100 number of fibers

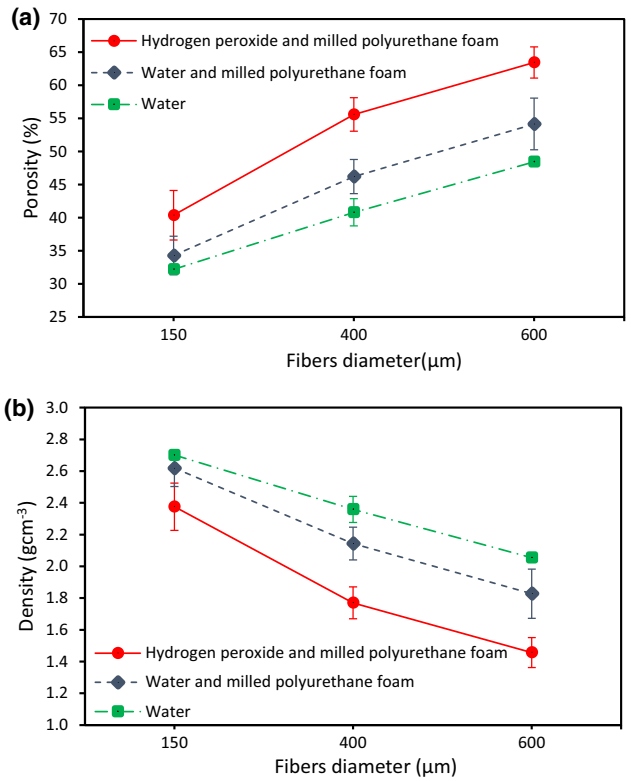

Fig. 7 **a** Porosity and **b** density of the scaffolds versus the fibers diameter with 90–100 number of fibers

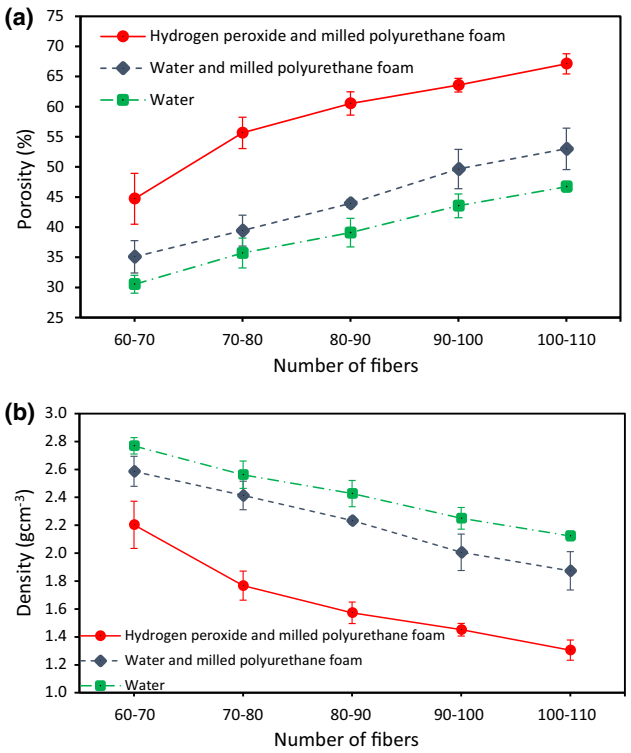

Fig. 8 **a** Porosity and **b** density of the scaffolds versus the number of fibers with 400 µm of diameter

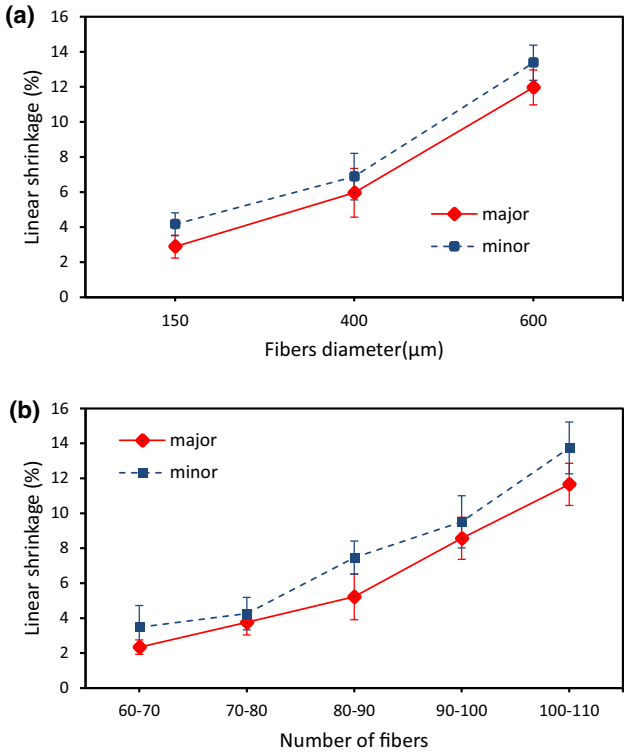

Fig. 9 Linear shrinkage of the scaffolds versus **a** the fibers diameter and **b** number of fibers with 400 μm of diameter

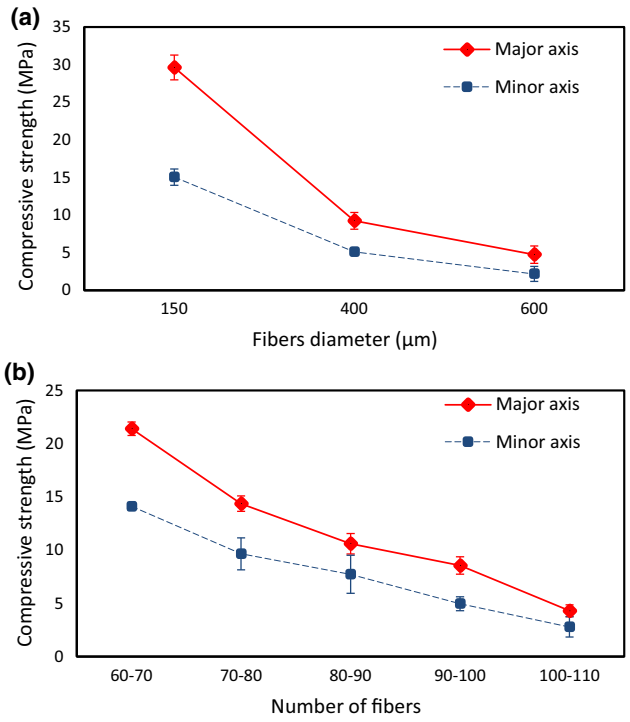

Fig. 10 Compressive strength of the scaffolds versus **a** the fibers diameter and **b** number of fibers with 400 μm of diameter

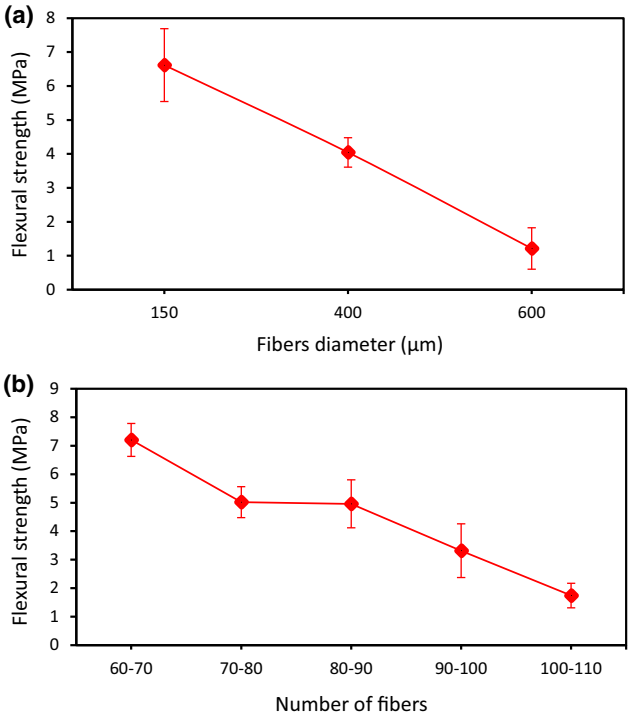

Fig. 11 Flexural strength of the scaffolds versus **a** the fibers diameter and **b** number of fibers with 400 μm of diameter

fabricated. The use of the hydrogen peroxide media and milled polyurethane foam addition resulted to the highest porosity values. So, this condition was selected for remained experiments.

The linear shrinkage of the scaffolds versus the diameter and number of fibers in the aligned oriented pore (major) and transverse (minor) directions is shown in Fig. 9. As illustrated, the shrinkage in the perpendicular direction to the aligned pores (radius direction) is more than that of axial direction because partial pressure of the material above a radius concave surface is lower than an axially distributed flat surface, and also vacancy concentration under a radius concave surface is greater than that under the axially distributed flat surface [26]; therefore, the rate of vacancy diffusion (i.e., pore removal) in radius direction is more than that of axial direction. It is noteworthy to emphasize that pores are vacancy source in sintering of materials. Considering porosity and shrinkage curves (Figs. 7, 8, 9) revealed that the scaffolds with higher porosity values were subjected to more shrinkage due to considerable pore removal during the progress of sintering process.

Figures 10 and 11 show the compressive and flexural strengths of the scaffolds as a function of the fibers diameter and number in the aligned oriented pores direc-

tion and transverse direction, respectively. As expected, similar to the density curves, compressive and flexural strengths showed a reverse relationship with the fibers diameter and number. An anisotropy in mechanical behaviors can be observed such that higher strengths in the aligned oriented pores direction than that of transverse were obtained. It is due to the anisotropic stress concentration on the scaffolds in different directions.

In the case of cancellous bone, anisotropic mechanical behavior with a strength of 5–10 MPa and high porosity is desired [25]. Considering of these characteristics showed that fabrication of the porous scaffolds using 90–100 number of fibers with 400 μm of diameter may represent the scaffolds with high porosity (∼65 %) and appropriate strength (∼10 MPa). The surface area of this kind of scaffold was measured as 5.80 m^2 g^{-1} which was appropriate for the scaffolds and almost accordance with samples having such porosities [12].

4 Conclusions

The present work focused on the fabrication of porous alumina with double shape architecture, oriented and rounded pores by slip casting method that could have potential in bone tissue scaffold. The results, generally, show that the slip casting method using silk threads as the fugitive fiber is a simple suitable route for the fabrication of alumina porous scaffolds having aligned oriented pores. With the increasing the diameter and number of the fibers, the scaffolds samples with higher porosity (68 %) can be achieved which is appropriate for the scaffolds used for bone tissue engineering. Furthermore, employing fibers with 400 μm of diameter for the fabrication of the samples, the scaffolds evidenced porosity value equal to 65 % and compressive strength equal to about 10 MPa. In addition, the simultaneous presence of silk fibers and milled polyurethane particles led to form axially oriented tiny microtube pores and bulk distributed rounded pores and homogeneously distributed throughout the bulk of the samples. The present results suggest that selection of the fiber types and diameter as sacrificial templates and slurry medias are very important for improving the mechanical properties and porosity of porous scaffolds for bone tissue engineering.

References

1. X. Liu, M.N. Rahaman, Q. Fu, Oriented bioactive glass (13–93) scaffolds with controllable pore size by unidirectional freezing of camphene-based suspensions: microstructure and mechanical response. Acta Biomater. **7**(1), 406–416 (2011)
2. M. Saki, M.K. Narbat, A. Samadikuchaksaraei, H.B. Ghafouri, F. Gorjipour, Biocompatibility study of a hydroxyapatite-alumina and silicon carbide composite scaffold for bone tissue engineering. Yakhteh Med. J. **11**(1), 55–60 (2009)
3. E. Soh, E. Kolos, A.J. Ruys, Foamed high porosity alumina for use as a bone tissue scaffold. Ceram. Int. **41**(1), 1031–1047 (2015)
4. E.D. Maio, A. Salerno, S. Iannace, Scaffolds with tubular/isotropic bi-modal pore structures by gas foaming and fiber templating. Mater. Lett. **93**, 157–160 (2013)
5. L.M. Bellan, S.P. Singh, P.W. Henderson, T.J. Porri, H.G. Craighead, J.A. Spector, Fabrication of an artificial 3-dimensional vascular network using sacrificial sugar structures. Soft Matter **5**(7), 1354–1357 (2009)
6. A. Sannino, L. Silvestri, M. Madaghiele, B. Harley, I.V. Yannas, Modeling the fabrication process of micropatterned macromolecular scaffolds for peripheral nerve regeneration. J. Appl. Polym. Sci. **116**(4), 1879–1888 (2010)
7. W. Acchar, F.B.M. Souza, E.G. Ramalho, W.L. Torquato, Mechanical characterization of cellular ceramics. Mater. Sci. Eng. A **513–514**, 340–343 (2009)
8. S. Bose, J. Darsell, H.L. Hosick, L. Yang, Processing and characterization of porous alumina scaffolds. J. Mater. Sci.—Mater. Med. **13**, 23–28 (2002)
9. S. Bose, J. Darsell, M. Kintner, H. Hosick, Pore size and pore volume effects on alumina and TCP ceramic scaffolds. Mater. Sci. Eng. C **23**, 479–486 (2003)
10. P. Lemes-Rachadel, G.S. Garcia, R.A.F. Machado, D. Hotza, J.C.D. da Costa, Current developments of mixed conducting membranes on porous substrates. Mater. Res. **44**, 1439–1516 (2013)
11. T. Fukasawa, M. Ando, T. Ohji, S. Kanzaki, Synthesis of porous ceramics with complex pore structure by freeze-dry processing. J. Am. Ceram. Soc. **84**(1), 230–232 (2001)
12. M.J. Ghaderi, M. Shafiee Afarani, G. Roudini, Synthesis of alumina porous supports via different compaction routes: vibration and pressing. J. Chem. Technol. Metall. **48**(3), 289–295 (2013)
13. J.H. Eom, Y.W. Kim, S. Raju, Processing and properties of macroporous silicon carbide ceramics: a review. J. Asian Ceram. Soc. **1**, 220–242 (2013)
14. Y.S. Han, J.B. Li, Y.J. Chen, Fabrication of bimodal porous ceramics. Mater. Res. Bull. **38**, 373–379 (2003)
15. A. Erol, I. Yildiz, A. Yonetken, Production and characterization of alumina based ceramic filter by using simple sponge. Technology **14**(3), 75–81 (2011)
16. H. Wang, I. Sung, X. Li, D. Kim, Fabrication of porous SiC ceramics with special morphologies by sacrificing template method. J. Porous Mater. **11**, 265–271 (2004)
17. E.C. Hammel, O.L.R. Ighodaro, O.I. Okoli, Processing and properties of advanced porous ceramics: an application based review. Ceram. Int. **40**, 15351–15370 (2014)
18. T. Isobe, Y. Kameshima, A. Nakajima, K. Okada, Preparation and properties of porous alumina ceramics with unidirectionally oriented pores by extrusion method using a plastic substance as a pore former. J. Eur. Ceram. Soc. **27**, 61–66 (2007)
19. Q. Fu, M.N. Rahaman, B.S. Bal, R.F. Brown, In vitro cellular response to hydroxyapatite scaffolds with oriented pore architectures. Mater. Sci. Eng. C **29**, 2147–2153 (2009)
20. A. Hadi, S. Baghshahi, R. Emadi, S. Naghavi, Different pore size alumina foams and study of their physical and mechanical properties. Mater. Sci. Eng. **132**, 340–343 (2009)
21. Y.W. Moon, K.H. Shin, Y.H. Koh, W.Y. Choi, H.E. Kim, Porous alumina ceramics with highly aligned pores by heat-treating extruded alumina/camphene body at temperature near its solidification point. J. Eur. Ceram. Soc. **32**, 1029–1034 (2012)
22. T. Isobe, Y. Kameshima, A. Nakajima, K. Okada, Y. Hotta, Gas permeability and mechanical properties of porous alumina

ceramics with unidirectionally aligned pores. J. Eur. Ceram. Soc. **27**, 53–59 (2007)
23. S. Jia, L. Liu, W. Pan, G. Meng, Ch. Duan, L. Zhang, Zh Xiong, J. Liu, Oriented cartilage extracellular matrix-derived scaffold for cartilage tissue engineering. J. Biosci. Bioeng. **113**, 647–653 (2012)
24. B.D. Boyan, T.W. Hummert, D.D. Dean, Z. Schwartz, Role of material surfaces in regulating bone and cartilage cell response. Biomaterials **17**, 137–146 (1996)
25. L.M. Mathieu, T.L. Mueller, P.E. Bourban, D.P. Pioletti, R. Muller, J.A.E. Manson, Architecture and properties of anisotropic polymer composite scaffolds for bone tissue engineering. Biomaterials **27**, 905–916 (2006)
26. M.W. Barsoum, *Fundamentals of Ceramics* (IoP, Bristol, 2003), pp. 311–313. **(chapter 10)**